

A Novel Joint Compressive Single Target Detection and Parameter Estimation in Radar without Signal Reconstruction

Alireza Hariri, Massoud Babaie-Zadeh

Department of Electrical Engineering, Sharif University of Technology, Tehran, Iran

E-mail: alireza.hariri1@gmail.com, mbzadeh@yahoo.com

Abstract—In this paper, a detector/estimator is proposed for compressed sensing radars, which does not need to reconstruct the radar signal, and which works directly from compressive measurements. More precisely, through direct processing of the measurements, and without the need for reconstructing the original radar signal, the system performs target detection, and then estimates range, Doppler frequency shift, and radar cross section in the presence of a Gaussian clutter. It can be seen that for large compression ratios, the detection performance and estimation quality is comparable to a common radar system while having a much lower data rate and with less computational load.

Index Terms—compressed sensing, detection-estimation, generalized likelihood ratio test, receiver operating characteristic, traditional radar system, compression ratio.

I. INTRODUCTION

APPLICATION of compressed sensing (CS) in radar signal processing has recently attracted the attention of many researchers [1], [2], [3], [4], [5], [6] because radar signals usually have high bandwidths at high carrier frequencies. Therefore, even when using bandpass sampling theorem [7], in order to have the signal not aliased, it is necessary to sample at a very high rate, leading to huge amounts of data. On the other hand, it is well-known in the CS literature [8], [9], [10] that one can take many fewer measurements (compared to Nyquist samples), without any loss of information.

Radar signal is generally sparse in the delay-Doppler domain [6] and CS theory may therefore be used to achieve more efficiency in storage space and computation time. On this basis, many works have been done in synthetic aperture radar (SAR) raw data processing to get its image with less need for onboard data storing and processing [1], [2], [3]. Recently, CS has been employed in multiple input multiple output (MIMO) radars to achieve more efficient processing of jointly received signals in order to detect targets and estimate their parameters, such as position and velocity [4], [5], [6].

In all of the above mentioned works, the desired signal used for detection and/or estimation is first reconstructed by using a general-purpose CS reconstruction algorithm [for example Orthogonal Matching Pursuit (OMP) [11], Basis Pursuit De-Noiseing (BPDN) or Compressive Sampling Matching Pursuit (CoSaMP) [12]] or an algorithm developed specially for the

specific problem [5], [13], [14]. However, the need for reconstructing the original signal for detection/estimation creates some difficulties. When using compressed sensing, the data rate is highly reduced, that is, the rate of measurements is much lower than for Nyquist samples. If, for processing the measurements, one needs to reconstruct the original signal, that is, reconstruct the Nyquist samples in some part of the system, then the data rate in that part is again very high. Therefore, it is desirable for detection/estimation to be based on directly processing the CS measurements, that is, by performing the processing within the CS “domain”. This has been the subject of some recent studies [15] and [16].

Detection/Estimation using CS measurements without reconstructing the original signal has been also discussed in fields other than radar. For example, authors in [17] and [18] studied blind communications in the CS domain. In [17], the carrier frequency of a blind phase shift keying (PSK) signal is estimated, which is a preliminary step for the modulation order estimation and blind signal detection. In [18], the unknown signal is classified between four modulations, namely Binary PSK (BPSK), Quadrature PSK (QPSK), 8PSK and 16 Quadrature Amplitude Modulation (16QAM). Detection, classification, estimation and filtering in the CS domain have been explored extensively in [15]. In fact, these were investigated for the most general form of the signal, and proper bounds (lower, upper or both) were introduced for the parameters determined for the algorithm qualification in each process. The bounds were derived based on the measurement matrix properties defined there. Authors in [16] proposed the idea for radar applications generally, but they followed it for Space Time Adaptive Processing (STAP). They then showed that statistical testing in the CS domain (compressive statistical testing) could perform at a level close to the traditional method for a sufficient number of measurements.

In this paper, detection/estimation in the CS domain is studied for a simple radar application. More precisely, the aim is to detect whether any target exists and, if yes, to estimate its parameters, such as range, Doppler frequency shift and radar cross section (RCS). It will be shown experimentally that an excellent detection-estimation performance can be obtained without the need for a lot of measurements (as is required in [16]). Therefore, even though the data rate of this new system is much lower than that of a common radar system, it is possible to achieve comparable qualities with less

computational load.

The paper is organized as follows. In Section II, the problem is defined and modeled mathematically. Section III is dedicated to solving problem. The performance of the proposed detection algorithm is given in Section IV. In Section V, the signal to noise and clutter ratio (SNCR) at the input and output of the measurement obtainer system is calculated, in order to restate the results of Section IV in terms of SCNR. Finally, the simulations and their results are described in Section VI.

Notations: For any vector \mathbf{y} , its transpose conjugate (Hermitian) is shown by \mathbf{y}^H . For any square matrix \mathbf{A} , its determinant is denoted by $|\mathbf{A}|$. \mathbf{I} is the identity matrix with appropriate dimensions. For any complex scalar a , its complex conjugate and real part are represented by a^* and $\Re\{a\}$ respectively. Finally, $\mathbb{E}\{\cdot\}$ stands for the expectation operator.

II. PROBLEM STATEMENT

Consider a scenario in which there is a target having unknown distance and velocity relative to the radar platform in the presence of clutter. As in [19], it is assumed that the clutter probability density function (PDF) is Gaussian and also that the radar pulse repetition frequency (PRF) is so high that the target's relative distance and velocity are nearly constant during different pulses. Furthermore, the target RCS is considered as a random variable and it is assumed that its value is constant throughout different pulses (called Swerling Case 1 in [20]). The received signal is sparse in time and in delay-Doppler domains [6], so instead of sampling the received signal at the Nyquist rate, it provides many fewer measurements with properties mentioned in the CS literatures [8].

The detection problem can be modeled in the form of a hypothesis testing problem as

$$\begin{cases} H_0 : \mathbf{y} = \Phi(\mathbf{c} + \mathbf{n}) \\ H_1 : \mathbf{y} = \Phi(\alpha \mathbf{s}_r(\tau, f_d) + \mathbf{c} + \mathbf{n}), \end{cases} \quad (1)$$

in which $\mathbf{y}_{M \times 1}$ is the measurements vector, $\Phi_{M \times N}$ is the real random Gaussian measurement matrix with independent identically distributed (i.i.d.) elements having zero mean and unit variance and $M \ll N$. It should be noted that the measurement matrix is assumed to be incoherent with time or delay-Doppler domain in which the received signal is sparse. $\mathbf{c}_{N \times 1}$ is the vector of clutter samples, $\mathbf{n}_{N \times 1}$ models the additive white Gaussian noise (AWGN) with variance σ_n^2 at the receiver, α is the complex RCS of the target, and $\mathbf{s}_r(\tau, f_d)$ is the received signal with delay τ and Doppler frequency shift f_d relative to the sent signal. As in [19], it is assumed that the distribution of \mathbf{c} is circular normal with zero mean and covariance matrix \mathbf{R}_c denoted as $\mathcal{CN}(\mathbf{0}, \mathbf{R}_c)$. As well, there is a pre-estimation of \mathbf{R}_c . Therefore, if the clutter to noise ratio (CNR) is fixed, σ_n^2 will be known. As mentioned in [20], circular normal distribution can be considered for α as $\mathcal{CN}(0, \sigma_\alpha^2)$, where σ_α^2 is its variance. This is because α is formed by the many scatterers in the target range-Doppler cell. Moreover, as in [21], and [22], it is assumed that σ_α^2 is known *a priori*.

The goal is to detect whether or not any target exists, and if yes, to estimate its parameters, namely range (or equivalently, delay), Doppler frequency shift and RCS.

III. THE PROBLEM SOLUTION

If the target exists, its range and Doppler frequency shift are not known *a priori*, so the usual likelihood ratio test (LRT) cannot be computed and used for the detection. Instead, the generalized likelihood ratio test (GLRT) should be used, in which the LRT is maximized to find the optimum delay (or equivalently, range) and Doppler frequency shift, which are also estimations of the supposed target's parameters. The LRT value at the optimal point should then be compared with a proper threshold. So at the first step, the PDF of the measurements vector for the two hypotheses is computed. Because noise and clutter vectors both have circular normal distribution, conditioned on H_0 , \mathbf{y} is a vector with distribution $\mathcal{CN}(\mathbf{0}, \Phi(\sigma_n^2 \mathbf{I} + \mathbf{R}_c) \Phi^T)$. If \mathbf{A} is defined as the covariance matrix of $\mathbf{y}|H_0$, for the null hypothesis, we have [23]

$$f(\mathbf{y}|H_0) = \frac{1}{\pi^M |\mathbf{A}|} \exp\{-\mathbf{y}^H \mathbf{A}^{-1} \mathbf{y}\}, \quad (2)$$

in which $\mathbf{A} = \sigma_n^2 \Phi \Phi^T + \Phi \mathbf{R}_c \Phi^T$. Similarly for the other hypothesis H_1 ,

$$f(\mathbf{y}|H_1, \alpha, \tau, f_d) = \mathcal{CN}(\alpha \Phi \mathbf{s}_r(\tau, f_d), \mathbf{A}) \quad (3)$$

$$= \frac{1}{\pi^M |\mathbf{A}|} \exp\left\{-\left(\mathbf{y} - \alpha \Phi \mathbf{s}_r(\tau, f_d)\right)^H \times \mathbf{A}^{-1} \left(\mathbf{y} - \alpha \Phi \mathbf{s}_r(\tau, f_d)\right)\right\}. \quad (4)$$

As was assumed in Section II, the distribution of α is $f_\alpha(\alpha) = \frac{1}{\pi \sigma_\alpha^2} \exp\left\{-\frac{|\alpha|^2}{\sigma_\alpha^2}\right\}$, and it is shown in A that $f(\mathbf{y}|H_1, \tau, f_d)$ is as

$$\begin{aligned} f(\mathbf{y}|H_1, \tau, f_d) &= \frac{1}{\pi^M |\mathbf{A}|} \exp\left\{-\mathbf{y}^H \mathbf{A}^{-1} \mathbf{y}\right\} \\ &\times \frac{1}{a(\tau, f_d) \sigma_\alpha^2 + 1} \exp\left\{\frac{b(\tau, f_d) \sigma_\alpha^2}{a(\tau, f_d) \sigma_\alpha^2 + 1}\right\}, \end{aligned} \quad (5)$$

where $a(\tau, f_d) = \mathbf{s}_r(\tau, f_d)^H \Phi^T \mathbf{A}^{-1} \Phi \mathbf{s}_r(\tau, f_d)$ and $b(\tau, f_d) = \left|\mathbf{y}^H \mathbf{A}^{-1} \Phi \mathbf{s}_r(\tau, f_d)\right|^2$. The LRT can then be derived as

$$\begin{aligned} \mathbf{L}(\mathbf{y}|\tau, f_d) &= \frac{f(\mathbf{y}|H_1, \tau, f_d)}{f(\mathbf{y}|H_0)} \\ &= \frac{1}{a(\tau, f_d) \sigma_\alpha^2 + 1} \exp\left\{\frac{b(\tau, f_d) \sigma_\alpha^2}{a(\tau, f_d) \sigma_\alpha^2 + 1}\right\}. \end{aligned} \quad (6)$$

In order to find the GLRT, $\mathbf{L}(\mathbf{y}|\tau, f_d)$ should be maximized over τ and f_d i.e.

$$\text{GLRT}(\mathbf{y}) = \max_{(\tau, f_d)} \mathbf{L}(\mathbf{y}|\tau, f_d). \quad (7)$$

As described in B, the GLRT will be in the form

$$\begin{aligned} \text{GLRT}(\mathbf{y}) &= \mathbf{L}(\mathbf{y}|\hat{\tau}, \hat{f}_d) \\ &= \sqrt{b(\hat{\tau}, \hat{f}_d)} \\ &= \left|\mathbf{y}^H \mathbf{A}^{-1} \Phi \mathbf{s}_r(\hat{\tau}, \hat{f}_d)\right| \geq \text{Th}, \end{aligned} \quad (8)$$

in which $(\hat{\tau}, \hat{f}_d) = \arg \max_{(\tau, f_d)} \mathbf{L}(\mathbf{y}|\tau, f_d)$, $1 - p_0$ is the *a priori* probability of the target existence and

$$\text{Th} = \frac{\sqrt{a(\hat{\tau}, \hat{f}_d)\sigma_\alpha^2 + 1}}{\sigma_\alpha} \sqrt{\ln \left(\frac{p_0}{1 - p_0} (a(\hat{\tau}, \hat{f}_d)\sigma_\alpha^2 + 1) \right)}. \quad (9)$$

IV. DETECTOR PERFORMANCE

For evaluating the detector performance, the receiver operating characteristic (ROC) curve, i.e. the detection probability (p_d) versus the false alarm probability (p_f), should be calculated. By defining $z \triangleq \mathbf{y}^H \mathbf{A}^{-1} \Phi \mathbf{s}_r(\hat{\tau}, \hat{f}_d)$, its PDF conditioned on the null hypothesis is

$$f(z|H_0) = \mathcal{CN}(0, a(\hat{\tau}, \hat{f}_d)). \quad (10)$$

So p_f is calculated as

$$\begin{aligned} p_f &= p(|z| > \text{Th}|H_0) \\ &= \int_{\text{Th}}^{\infty} p_x(x|H_0) dx \\ &= 1 - \int_{-\infty}^{\text{Th}} p_x(x|H_0) dx \\ &= \exp \left\{ -\frac{\text{Th}^2}{a(\hat{\tau}, \hat{f}_d)} \right\}, \end{aligned} \quad (11)$$

in which $x = |z|$ has a Rayleigh distribution with parameter $(a(\hat{\tau}, \hat{f}_d)/2)^{1/2}$ conditioned on H_0 , denoted as $\text{Ray}((a(\hat{\tau}, \hat{f}_d)/2)^{1/2})$ [24].

On the other hand, the PDF of z conditioned on H_1 and α can be written as

$$f(z|H_1, \alpha) = \mathcal{CN}(\alpha a(\hat{\tau}, \hat{f}_d), a(\hat{\tau}, \hat{f}_d)). \quad (12)$$

If the above PDF is averaged over α , as shown in C, $f(z|H_1)$ will be as

$$f(z|H_1) = \mathcal{CN}(0, a(\hat{\tau}, \hat{f}_d) + a(\hat{\tau}, \hat{f}_d)^2 \sigma_\alpha^2). \quad (13)$$

Therefore p_d will be

$$\begin{aligned} p_d &= p(|z| > \text{Th}|H_1) \\ &= \int_{\text{Th}}^{\infty} p_x(x|H_1) dx \\ &= 1 - \int_{-\infty}^{\text{Th}} p_x(x|H_1) dx \\ &= \exp \left\{ -\frac{\text{Th}^2}{a(\hat{\tau}, \hat{f}_d) + a(\hat{\tau}, \hat{f}_d)^2 \sigma_\alpha^2} \right\}, \end{aligned} \quad (14)$$

where, similar to the H_0 hypothesis, $p_x(x|H_1) = \text{Ray}(((a(\hat{\tau}, \hat{f}_d) + a(\hat{\tau}, \hat{f}_d)^2 \sigma_\alpha^2)/2)^{1/2})$.

In order to obtain the ROC, it can be seen from (11) that $\text{Th}^2 = -a(\hat{\tau}, \hat{f}_d) \ln p_f$ so $p_d = \exp \left\{ \frac{a(\hat{\tau}, \hat{f}_d) \ln p_f}{a(\hat{\tau}, \hat{f}_d) + a(\hat{\tau}, \hat{f}_d)^2 \sigma_\alpha^2} \right\}$ or in other words

$$p_d = p_f \left(1 + a(\hat{\tau}, \hat{f}_d) \sigma_\alpha^2 \right)^{-1}. \quad (15)$$

V. SNCR AT THE MEASUREMENTS' OBTAINER SYSTEM

INPUT AND OUTPUT

The signal at the input of the measurements' obtainer system is $\mathbf{y}_{in} = \alpha \mathbf{s}_r(\tau, f_d) + \mathbf{c} + \mathbf{n}$. The signal term is $\alpha \mathbf{s}_r(\tau, f_d)$ and the noise-clutter term is $\mathbf{c} + \mathbf{n}$. Therefore, the signal power is $\mathbb{E} \left\{ \|\alpha \mathbf{s}_r(\tau, f_d)\|_2^2 \right\} = \sigma_\alpha^2 N_p P_w$, where N_p is the number of pulses sent and P_w is the number of samples in a pulse. Here it is assumed that the pulses are rectangular. On the other hand, the noise-clutter power is $\mathbb{E} \left\{ \|\mathbf{c} + \mathbf{n}\|_2^2 \right\}$. Because the noise and clutter are statistically independent, it can be written as

$$\mathbb{E} \left\{ \|\mathbf{c} + \mathbf{n}\|_2^2 \right\} = \mathbb{E} \left\{ \|\mathbf{c}\|_2^2 \right\} + \mathbb{E} \left\{ \|\mathbf{n}\|_2^2 \right\} = \sum_{i=1}^N \lambda_i + N \sigma_n^2, \quad (16)$$

where λ_i s are the eigenvalues of \mathbf{R}_c . Therefore, the input SNCR will be

$$\text{SNCR}_{\text{in}} = \frac{\sigma_\alpha^2 N_p P_w}{N \sigma_n^2 + \sum_{i=1}^N \lambda_i}. \quad (17)$$

As derived in (8), the output statistic for GLRT is

$$\begin{aligned} x &= \left| \mathbf{y}^H \mathbf{A}^{-1} \Phi \mathbf{s}_r(\hat{\tau}, \hat{f}_d) \right| \\ &= \left| \mathbf{s}_r(\hat{\tau}, \hat{f}_d)^H \Phi^T \mathbf{A}^{-1} \mathbf{y} \right| \\ &= \left| \alpha \mathbf{s}_r(\hat{\tau}, \hat{f}_d)^H \Phi^T \mathbf{A}^{-1} \Phi \mathbf{s}_r(\hat{\tau}, \hat{f}_d) \right. \\ &\quad \left. + \mathbf{s}_r(\hat{\tau}, \hat{f}_d)^H \Phi^T \mathbf{A}^{-1} \Phi (\mathbf{c} + \mathbf{n}) \right| \\ &= \left| \alpha a(\hat{\tau}, \hat{f}_d) + \mathbf{s}_r(\hat{\tau}, \hat{f}_d)^H \Phi^T \mathbf{A}^{-1} \Phi (\mathbf{c} + \mathbf{n}) \right|. \end{aligned} \quad (18)$$

Therefore, x^2 can be expanded as

$$\begin{aligned} x^2 &= |\alpha|^2 a(\hat{\tau}, \hat{f}_d)^2 \\ &\quad + \alpha^* a(\hat{\tau}, \hat{f}_d) \mathbf{s}_r(\hat{\tau}, \hat{f}_d)^H \Phi^T \mathbf{A}^{-1} \Phi (\mathbf{c} + \mathbf{n}) \\ &\quad + \alpha a(\hat{\tau}, \hat{f}_d) (\mathbf{c} + \mathbf{n})^H \Phi^T \mathbf{A}^{-1} \Phi \mathbf{s}_r(\hat{\tau}, \hat{f}_d) \\ &\quad + \mathbf{s}_r(\hat{\tau}, \hat{f}_d)^H \Phi^T \mathbf{A}^{-1} \Phi (\mathbf{c} + \mathbf{n}) \\ &\quad \times (\mathbf{c} + \mathbf{n})^H \Phi^T \mathbf{A}^{-1} \Phi \mathbf{s}_r(\hat{\tau}, \hat{f}_d). \end{aligned} \quad (19)$$

If the input SNCR is high, it can be assumed that $\|\alpha \mathbf{s}_r(\hat{\tau}, \hat{f}_d)\|_2 \gg \|\mathbf{c} + \mathbf{n}\|_2$. Then, x can be approximated as

$$\begin{aligned} x &= |\alpha| a(\hat{\tau}, \hat{f}_d) \left(1 + \frac{\mathbf{s}_r(\hat{\tau}, \hat{f}_d)^H \Phi^T \mathbf{A}^{-1} \Phi (\mathbf{c} + \mathbf{n})}{\alpha a(\hat{\tau}, \hat{f}_d)} \right. \\ &\quad \left. + \frac{(\mathbf{c} + \mathbf{n})^H \Phi^T \mathbf{A}^{-1} \Phi \mathbf{s}_r(\hat{\tau}, \hat{f}_d)}{\alpha^* a(\hat{\tau}, \hat{f}_d)} \right. \\ &\quad \left. + \mathbf{s}_r(\hat{\tau}, \hat{f}_d)^H \Phi^T \mathbf{A}^{-1} \Phi (\mathbf{c} + \mathbf{n}) \right. \\ &\quad \left. \times \frac{(\mathbf{c} + \mathbf{n})^H \Phi^T \mathbf{A}^{-1} \Phi \mathbf{s}_r(\hat{\tau}, \hat{f}_d)}{|\alpha|^2 a(\hat{\tau}, \hat{f}_d)^2} \right)^{1/2} \\ &\cong |\alpha| a(\hat{\tau}, \hat{f}_d) \left(1 + \frac{\mathbf{s}_r(\hat{\tau}, \hat{f}_d)^H \Phi^T \mathbf{A}^{-1} \Phi (\mathbf{c} + \mathbf{n})}{\alpha a(\hat{\tau}, \hat{f}_d)} \right. \\ &\quad \left. + \frac{(\mathbf{c} + \mathbf{n})^H \Phi^T \mathbf{A}^{-1} \Phi \mathbf{s}_r(\hat{\tau}, \hat{f}_d)}{\alpha^* a(\hat{\tau}, \hat{f}_d)} \right)^{1/2} \end{aligned}$$

$$\begin{aligned}
&= |\alpha| a(\hat{\tau}, \hat{f}_d) \sqrt{1 + 2\Re\left\{\frac{\mathbf{s}_r(\hat{\tau}, \hat{f}_d)^H \Phi^T \mathbf{A}^{-1} \Phi (\mathbf{c} + \mathbf{n})}{\alpha a(\hat{\tau}, \hat{f}_d)}\right\}} \\
&\cong |\alpha| a(\hat{\tau}, \hat{f}_d) \left(1 + \Re\left\{\frac{\mathbf{s}_r(\hat{\tau}, \hat{f}_d)^H \Phi^T \mathbf{A}^{-1} \Phi (\mathbf{c} + \mathbf{n})}{\alpha a(\hat{\tau}, \hat{f}_d)}\right\}\right) \\
&= |\alpha| a(\hat{\tau}, \hat{f}_d) + \Re\left\{\frac{|\alpha|}{\alpha} \mathbf{s}_r(\hat{\tau}, \hat{f}_d)^H \Phi^T \mathbf{A}^{-1} \Phi (\mathbf{c} + \mathbf{n})\right\}. \tag{20}
\end{aligned}$$

If α is considered in the polar form as $\alpha = |\alpha|e^{j\psi}$, x can be written as

$$\begin{aligned}
x &= |\alpha| a(\hat{\tau}, \hat{f}_d) \\
&\quad + \Re\left\{e^{-j\psi} \mathbf{s}_r(\hat{\tau}, \hat{f}_d)^H \Phi^T \mathbf{A}^{-1} \Phi (\mathbf{c} + \mathbf{n})\right\}. \tag{21}
\end{aligned}$$

In (21), the signal term is $|\alpha| a(\hat{\tau}, \hat{f}_d)$ and the noise-clutter term is $\Re\left\{e^{-j\psi} \mathbf{s}_r(\hat{\tau}, \hat{f}_d)^H \Phi^T \mathbf{A}^{-1} \Phi (\mathbf{c} + \mathbf{n})\right\}$. Therefore, the signal power is $a(\hat{\tau}, \hat{f}_d)^2 \sigma_\alpha^2$. For the noise-clutter power calculation, s is defined as $s \triangleq \mathbf{s}_r(\hat{\tau}, \hat{f}_d)^H \Phi^T \mathbf{A}^{-1} \Phi (\mathbf{c} + \mathbf{n})$ so the noise-clutter term (NCT) can be restated as

$$\begin{aligned}
\text{NCT} &= \Re\left\{e^{-j\psi} \mathbf{s}_r(\hat{\tau}, \hat{f}_d)^H \Phi^T \mathbf{A}^{-1} \Phi (\mathbf{c} + \mathbf{n})\right\} \\
&= \Re\{s e^{-j\psi}\} \\
&= s_r \cos \psi + s_i \sin \psi, \tag{22}
\end{aligned}$$

where s_r and s_i are the real and imaginary parts of s respectively. The noise-clutter power will be

$$\begin{aligned}
\mathbb{E}\{(s_r \cos \psi + s_i \sin \psi)^2\} &= \mathbb{E}\{s_r^2 \cos^2 \psi + s_i^2 \sin^2 \psi \\
&\quad + 2s_r s_i \cos \psi \sin \psi\} \\
&= \mathbb{E}\{s_r^2 \cos^2 \psi + s_i^2 \sin^2 \psi\},
\end{aligned}$$

because \mathbf{c} and \mathbf{n} are circular normal and independent of each other, s is circular normal and therefore its real and imaginary parts are statistically independent and both are zero-mean. Furthermore, s is independent of ψ , which has a uniform distribution in the interval $[0, 2\pi)$, so

$$\text{NCP} = \frac{1}{2} \mathbb{E}\{s_r^2 + s_i^2\} = \frac{1}{2} \mathbb{E}\{|s|^2\} = \frac{1}{2} a(\hat{\tau}, \hat{f}_d)^2, \tag{23}$$

where NCP stands for noise-clutter power. From (23), it can be concluded that

$$\text{SNCR}_{\text{out}} = 2\sigma_\alpha^2 a(\hat{\tau}, \hat{f}_d)^2, \tag{24}$$

which can be written from (15) in terms of the detection and false alarm probability as

$$\text{SNCR}_{\text{out}} = 2 \left(\frac{\ln p_f}{\ln p_d} - 1 \right). \tag{25}$$

VI. RESULTS AND SIMULATIONS

In this section, five simulations are conducted to experimentally evaluate the performance of the proposed detection-estimation approach. In all of these simulations, the target RCS, its distance and speed relative to the radar, CNR and also the number of samples are fixed as $\text{RCS} = 10.16$, $R = 3900\text{m}$, $v = 198\text{m/s}$, $\text{CNR} = 27\text{dB}$ and $N = 1320$. In the following, compression ratio (CR) means the fraction $\frac{M}{N}$, and in the case $\frac{M}{N} = 1$, the measurement matrix is set to identity. In other

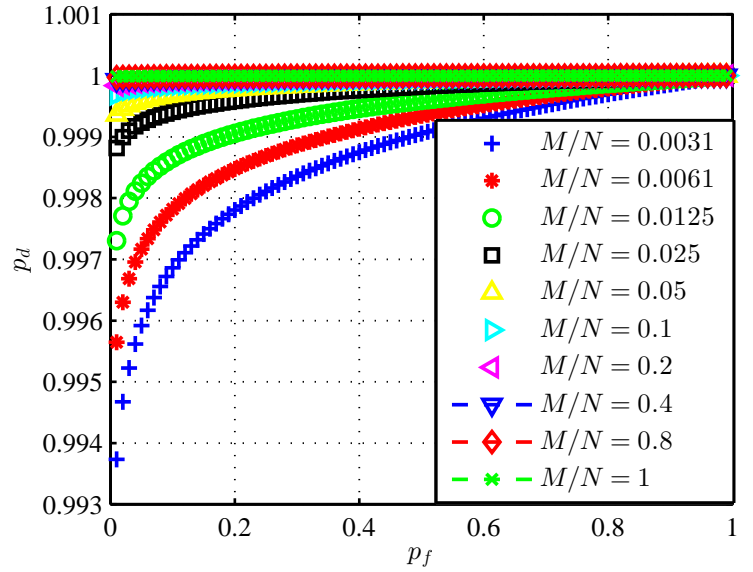


Fig. 1. ROC curves for different compression ratios at $\text{SNCR}_{\text{in}} = 20\text{dB}$ ($\frac{M}{N} = 1$ means a traditional radar system).

words, $\text{CR} = 1$ corresponds to the traditional radar system, which does not use CS.

Experiments 1, 2 and 3. Performance Analysis

In these experiments, the presented detector performance is studied and compared with the traditional method, by using (15). At first, SNCR_{in} is fixed at 20dB so by (17) σ_α^2 is known. The ROC curves for a fixed $\text{SNCR}_{\text{in}} = 20\text{dB}$ and for different CRs are plotted in Fig. 1. The chosen CRs (except 1) constitute a geometrical sequence with the first term 0.0031 and common ratio 2 to cover the interval $(0, 1)$ in a good manner. As can be seen, the lower the CR, the better the detector performance. This was expected because, by increasing the number of measurements, more information from the incoming signal is obtained. These curves show that the performance degradation is very small, even for $\text{CR} = 0.0031$ (the detection probability is above 0.99 for all false alarm probabilities). For comparison, the ROC curves for the CS method with reconstruction at $\text{SNCR}_{\text{in}} = 20\text{dB}$ are plotted in Fig. 2. The OMP algorithm is used for CS reconstruction. As it is observed, the detection is very good (the detection probability is near 0.99 for all false alarm probabilities).

Secondly, the detection probability has been shown versus CR for different input SNCRs at fixed false alarm probability $p_f = 10^{-4}$. Here, the input SNCR is varied to have a single target with different powers. For each one, p_d is then computed, while CR varies as the first simulation. The result is shown in Fig. 3. It is observed that, up to $\text{SNCR}_{\text{in}} = 15\text{dB}$, the obtained detection probability at the largest CR is above 0.95 for $p_f = 10^{-4}$.

In the third simulation, the ROC curve is derived for different input SNCRs at fixed $\text{CR} = 0.0031$. ROC curves for a fixed CR and for different input SNCRs, or equivalently different target powers, have been plotted in Fig. 4. From this figure, it can be deduced that, to have a good detection performance

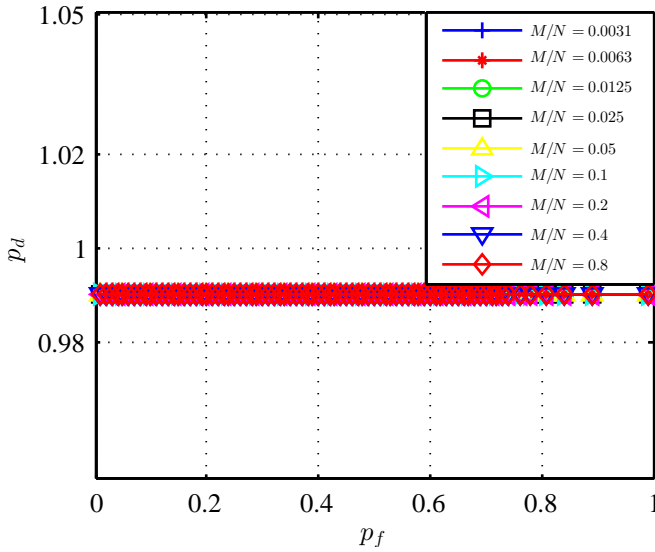


Fig. 2. ROC curves for different compression ratios at $\text{SNCR}_{in} = 20\text{dB}$ with CS reconstruction.

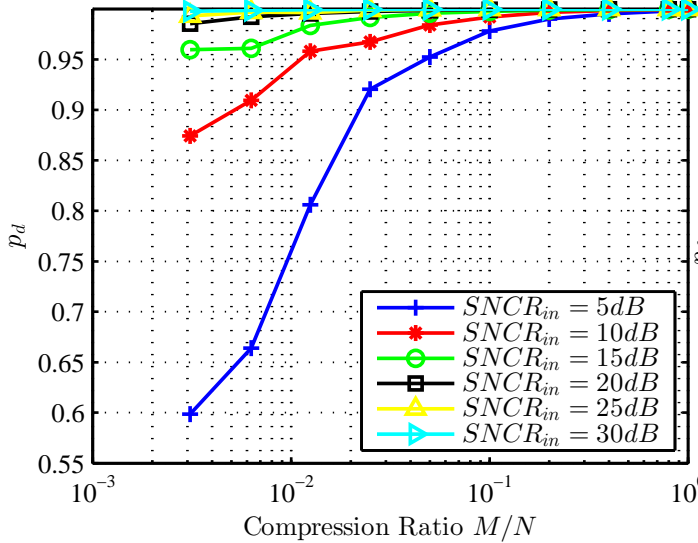


Fig. 3. Detection probability versus compression ratio for different input SNCRs at constant false alarm probability $p_f = 10^{-4}$ ($\frac{M}{N} = 1$ means a traditional radar system).

(detection probability above 0.97) at $\text{CR} = 0.0031$, the input SNCR should be increased to 15dB. This is not surprising, because the number of measurements has been reduced *very much*, so the input SNCR has to be increased *a little*. This is the key point: by increasing the input SNCR a little, with very few measurements, a very good performance can be obtained. For comparison, the ROC curves for the CS method with reconstruction at $\text{CR} = 0.0031$ are plotted in Fig. 5. It can be again seen that, to have an acceptable detection performance, the input SNCR should be increased.

Experiment 4. Computational Cost

In this experiment, the computational cost of the presented detector is studied and compared with the traditional radar

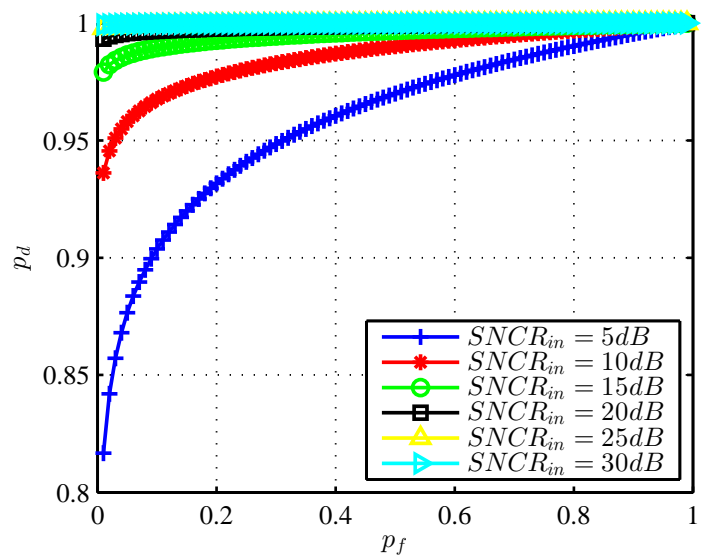


Fig. 4. The ROC curves for different input SNCRs at fixed compression ratio $\frac{M}{N} = 0.0031$

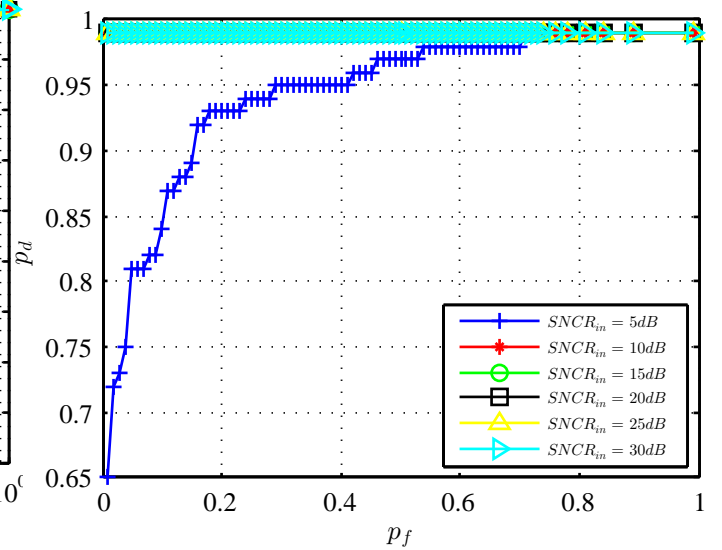


Fig. 5. The ROC curves for different input SNCRs at fixed compression ratio $\frac{M}{N} = 0.0031$ with CS reconstruction.

system, i.e. $\text{CR} = 1$. The averaged CPU time of the detection process over 100 simulations is used as a rough measure of the complexity of the detection algorithm for different CRs. Simulations are performed in MATLAB R2013a environment, using Intel Core (TM) 2 Duo P8800, 2.67GHz processor with 4GB of memory, and under 64 bit Microsoft Windows 7 operating system.

The results are shown in Fig. 6. It is seen that at $\text{CR} = 0.0031$, around 2% reduction in computational cost has been achieved. Contrary to previous compressive sensing radars [1], [2], [3], [4], [5], [6], this system does not reconstruct the Nyquist samples. So, as demonstrated in Figs. 1 and 4, having a data rate of only 0.3% of a common radar system, the detection probability is above 0.99, with about a 2% reduction

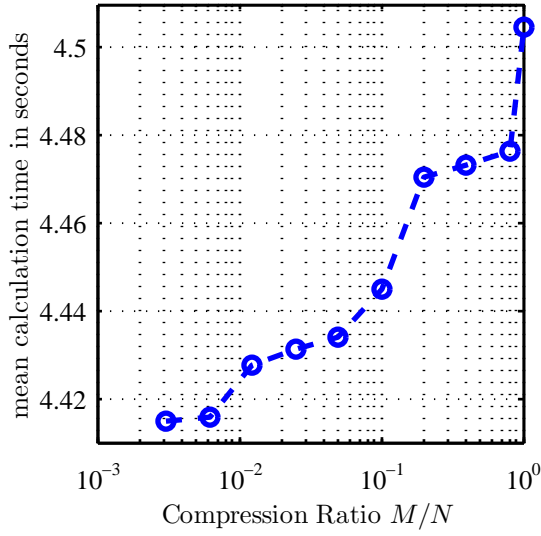


Fig. 6. The mean detection time in seconds versus compression ratio ($\frac{M}{N} = 1$ means a traditional radar system).

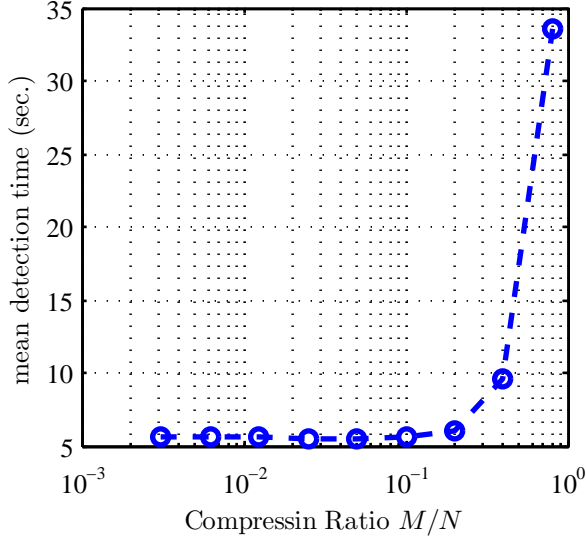


Fig. 7. The mean detection time in seconds versus compression ratio with CS reconstruction. The averaged CPU time is increased, however, the key point is that with CS reconstruction the data rate is increased.

in computational load. In Fig. 7, the mean detection time is plotted when CS reconstruction is used. As it is seen, the averaged CPU time is increased, however, the key point is that with CS reconstruction the data rate is increased.

Experiments 5, 6, and 7. Parameters Estimation Accuracy

In these three experiments, the estimation accuracy of the target parameters is studied. To estimate the target delay and Doppler frequency shift, (6) and (7) are used. In these experiments, the simulation is run 100 times and the mean and standard deviation of the estimated parameters computed. Input SNCR is varied from 5dB to 30dB. Figures 8 and 9 depict the estimated delay $\hat{\tau}$ and Doppler frequency shift \hat{f}_d respectively for different values of CR and input SNCR. It is interesting to note that even at $\text{SNCR}_{in} = 5\text{dB}$ for CRs less

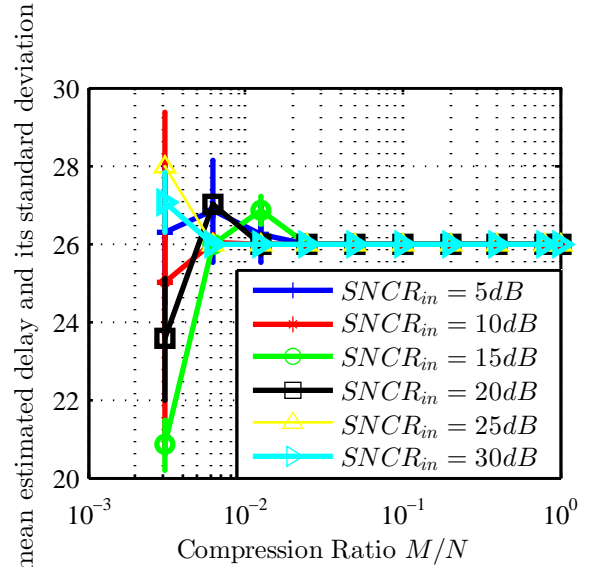


Fig. 8. Mean estimated delay ($\hat{\tau}$) and its standard deviation versus compression ratio for input SNCR varied from 5dB to 30dB (the true delay value is $\tau = 26$). Note: $\frac{M}{N} = 1$ means a traditional radar system.

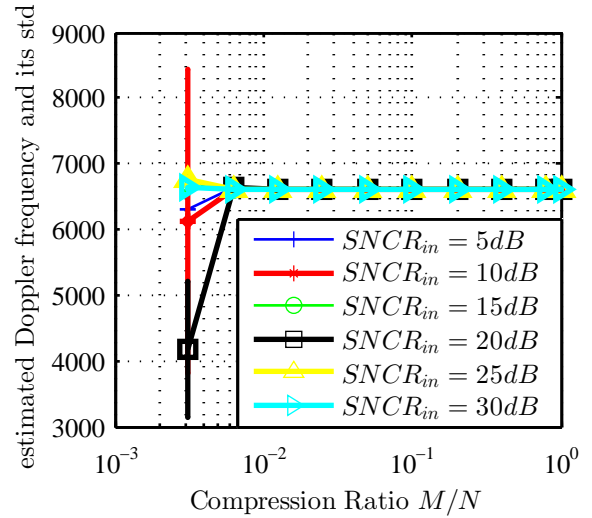


Fig. 9. Mean estimated Doppler frequency shift (\hat{f}_d) and its standard deviation versus compression ratio at for input SNCR varied from 5dB to 30dB (the true Doppler frequency shift value is $f_d = 6600$). Note: $\frac{M}{N} = 1$ means a traditional radar system.

than 0.0125, the standard deviation of the estimated delay is negligible, while using less than 2% of the samples of the traditional radar system. Similarly for the Doppler frequency shift estimation at CRs less than 0.0031, the standard deviation is very small. It should also be noted that although there are some errors in the estimated parameters for CRs greater than 0.0125, the detection performance is still good for input SNCRs greater than 10dB (the detection probability is above 0.95).

For signal modeling in the presence of a target, it was assumed that the signal complex RCS is a circular normal

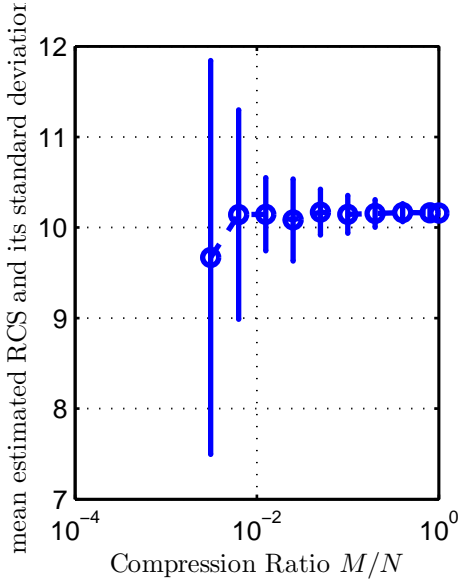


Fig. 10. Mean estimated RCS and its standard deviation versus compression ratio at $\text{SNCR}_{\text{in}} = 20\text{dB}$ (the true RCS value is 10.16). Note: $\frac{M}{N} = 1$ means a traditional radar system.

random variable. In practice, however, it can be estimated using the measurements vector. In fact, if the input SNCR is high, from (18) the target RCS can be approximated as

$$|\alpha| \cong \frac{|\mathbf{y}^H \mathbf{A}^{-1} \Phi \mathbf{s}_r(\hat{\tau}, \hat{f}_d)|}{\mathbf{s}_r(\hat{\tau}, \hat{f}_d)^H \Phi^T \mathbf{A}^{-1} \Phi \mathbf{s}_r(\hat{\tau}, \hat{f}_d)} = \frac{\sqrt{b(\hat{\tau}, \hat{f}_d)}}{a(\hat{\tau}, \hat{f}_d)}. \quad (26)$$

The RCS approximation accuracy is simulated similar to the delay and Doppler frequency shift at $\text{SNCR}_{\text{in}} = 20\text{dB}$. Figure 10 shows the results. For CRs less than 0.025, the error in the mean RCS approximation and the standard deviation is tolerable (less than 5%), but for CRs greater than 0.05, there may be a large error in the mean RCS approximation. Therefore, for RCS approximation, a few more measurements should be obtained.

VII. CONCLUSION

In this paper, it has been shown that a target can be detected in the presence of a Gaussian clutter, and its important parameters, such as range, Doppler frequency shift and RCS, can be estimated using compressive measurements without reconstructing Nyquist samples. In fact, by using very high compression ratios (like 0.0031), the detection performance is proper and the estimation quality is comparable to traditional radar systems while having a much lower data rate and with less computational load. So it seems that the proposed detection algorithm is very suitable especially for high pulse bandwidth radars.

APPENDIX A

PROOF OF (5)

It is obvious that

$$f(\mathbf{y}|H_1, \tau, f_d) = \int f(\mathbf{y}|H_1, \alpha, \tau, f_d) f_\alpha(\alpha) d\alpha_r d\alpha_i, \quad (27)$$

in which α_r and α_i are the real and imaginary parts of α , respectively. By substituting the distribution $f(\mathbf{y}|H_1, \alpha, \tau, f_d)$ from (4) in (27) and using $f_\alpha(\alpha) = \frac{1}{\pi\sigma_\alpha^2} \exp\left\{-\frac{|\alpha|^2}{\sigma_\alpha^2}\right\}$ we have

$$\begin{aligned} f(\mathbf{y}|H_1, \tau, f_d) &= \frac{1}{\pi^M |\mathbf{A}|} \frac{1}{\pi\sigma_\alpha^2} \exp\{-\mathbf{y}^H \mathbf{A}^{-1} \mathbf{y}\} \\ &\times \iint_{-\infty}^{\infty} \exp\{-\mathbf{s}_r(\tau, f_d)^H \Phi^T \mathbf{A}^{-1} \Phi \mathbf{s}_r(\tau, f_d) |\alpha|^2\} \\ &\times \exp\{\mathbf{s}_r(\tau, f_d)^H \Phi^T \mathbf{A}^{-1} \mathbf{y} \alpha^*\} \\ &\times \exp\{\mathbf{y}^H \mathbf{A}^{-1} \Phi \mathbf{s}_r(\tau, f_d) \alpha\} \exp\left\{-\frac{|\alpha|^2}{\sigma_\alpha^2}\right\} d\alpha_r d\alpha_i. \end{aligned}$$

If we define $a(\tau, f_d) \triangleq \mathbf{s}_r(\tau, f_d)^H \Phi^T \mathbf{A}^{-1} \Phi \mathbf{s}_r(\tau, f_d)$ (it is real valued because $a^*(\tau, f_d) = a(\tau, f_d)$) and $c(\tau, f_d) \triangleq \mathbf{s}_r(\tau, f_d)^H \Phi^T \mathbf{A}^{-1} \mathbf{y}$, it can be written

$$\begin{aligned} f(\mathbf{y}|H_1, \tau, f_d) &= \frac{1}{\pi^M |\mathbf{A}|} \frac{1}{\pi\sigma_\alpha^2} \exp\{-\mathbf{y}^H \mathbf{A}^{-1} \mathbf{y}\} \\ &\times \iint_{-\infty}^{\infty} \exp\left\{-\left(a(\tau, f_d) + \frac{1}{\sigma_\alpha^2}\right) |\alpha|^2\right\} \\ &\times \exp\{c(\tau, f_d) \alpha^* + c(\tau, f_d)^* \alpha\} d\alpha_r d\alpha_i \\ &= \frac{1}{\pi^M |\mathbf{A}|} \frac{1}{\pi\sigma_\alpha^2} \exp\{-\mathbf{y}^H \mathbf{A}^{-1} \mathbf{y}\} \\ &\times \iint_{-\infty}^{\infty} \exp\left\{-e(\tau, f_d) \left(|\alpha|^2 - \frac{c(\tau, f_d) \alpha^*}{e(\tau, f_d)}\right.\right. \\ &\quad \left.\left. - \frac{c(\tau, f_d)^* \alpha}{e(\tau, f_d)}\right)\right\} d\alpha_r d\alpha_i \\ &= \frac{1}{\pi^M |\mathbf{A}|} \frac{1}{\pi\sigma_\alpha^2} \exp\{-\mathbf{y}^H \mathbf{A}^{-1} \mathbf{y}\} \\ &\times \iint_{-\infty}^{\infty} \exp\left\{-e(\tau, f_d) \left(|\alpha - \frac{c(\tau, f_d)}{e(\tau, f_d)}\right|^2\right.\right. \\ &\quad \left.\left. - \frac{|c(\tau, f_d)|^2}{e(\tau, f_d)^2}\right)\right\} d\alpha_r d\alpha_i \\ &= \frac{1}{\pi^M |\mathbf{A}|} \frac{1}{\sigma_\alpha^2 e(\tau, f_d)} \exp\{-\mathbf{y}^H \mathbf{A}^{-1} \mathbf{y}\} \\ &\times \exp\left\{\frac{|c(\tau, f_d)|^2}{e(\tau, f_d)}\right\}. \quad (28) \end{aligned}$$

In (28), $e(\tau, f_d) = a(\tau, f_d) + \frac{1}{\sigma_\alpha^2}$ and the last equality is obtained by Gaussian PDF integration [25]. By defining $b(\tau, f_d) \triangleq |c(\tau, f_d)|^2 = |\mathbf{s}_r(\tau, f_d)^H \Phi^T \mathbf{A}^{-1} \mathbf{y}|^2$ it can be shown that

$$\begin{aligned} f(\mathbf{y}|H_1, \tau, f_d) &= \frac{1}{\pi^M |\mathbf{A}|} \frac{1}{\sigma_\alpha^2 a(\tau, f_d) + 1} \exp\{-\mathbf{y}^H \mathbf{A}^{-1} \mathbf{y}\} \\ &\times \exp\left\{\frac{\sigma_\alpha^2 b(\tau, f_d)}{\sigma_\alpha^2 a(\tau, f_d) + 1}\right\}, \quad (29) \end{aligned}$$

which is the same as (5).

APPENDIX B

PROOF OF (8)

According to (6) the likelihood ratio test is

$$\begin{aligned} \mathbf{L}(\mathbf{y}|\tau, f_d) &= \frac{1}{a(\tau, f_d)\sigma_\alpha^2 + 1} \exp\left\{\frac{b(\tau, f_d)\sigma_\alpha^2}{a(\tau, f_d)\sigma_\alpha^2 + 1}\right\}, \\ &\geq \frac{p_0}{1 - p_0} \end{aligned} \quad (30)$$

in which p_0 is the *a priori* probability of the H_0 hypothesis. As is obvious, $a(\tau, f_d)$ is not a function of observations (measurements). So the new likelihood ratio test can be reformulated as

$$\begin{aligned} \mathbf{L}_1(\mathbf{y}|\tau, f_d) &= \exp\left\{\frac{b(\tau, f_d)\sigma_\alpha^2}{a(\tau, f_d)\sigma_\alpha^2 + 1}\right\} \\ &\geq \frac{p_0}{1 - p_0} (a(\tau, f_d)\sigma_\alpha^2 + 1) \Rightarrow \\ \mathbf{L}_2(\mathbf{y}|\tau, f_d) &= \frac{b(\tau, f_d)\sigma_\alpha^2}{a(\tau, f_d)\sigma_\alpha^2 + 1} \\ &\geq \ln\left(\frac{p_0}{1 - p_0} (a(\tau, f_d)\sigma_\alpha^2 + 1)\right) \Rightarrow \\ \mathbf{L}_3(\mathbf{y}|\tau, f_d) &= b(\tau, f_d) \geq \frac{a(\tau, f_d)\sigma_\alpha^2 + 1}{\sigma_\alpha^2} \\ &\quad \times \ln\left(\frac{p_0}{1 - p_0} (a(\tau, f_d)\sigma_\alpha^2 + 1)\right) \Rightarrow \\ \mathbf{L}_4(\mathbf{y}|\tau, f_d) &= \sqrt{b(\tau, f_d)} = |\mathbf{s}_r(\tau, f_d)^H \mathbf{\Phi}^T \mathbf{A}^{-1} \mathbf{y}| \\ &\geq \frac{\sqrt{a(\tau, f_d)\sigma_\alpha^2 + 1}}{\sigma_\alpha} \\ &\quad \times \sqrt{\ln\left(\frac{p_0}{1 - p_0} (a(\tau, f_d)\sigma_\alpha^2 + 1)\right)}. \end{aligned} \quad (31)$$

If $\mathbf{L}_4(\mathbf{y}|\tau, f_d)$ is maximized over τ and f_d simultaneously, the GLRT will be $\text{GLRT}(\mathbf{y}) = \max_{(\tau, f_d)} \mathbf{L}_4(\mathbf{y}|\tau, f_d)$ in which $(\hat{\tau}, \hat{f}_d) = \arg \max_{(\tau, f_d)} \mathbf{L}_4(\mathbf{y}|\tau, f_d)$. This is exactly (7). So the GLRT can be written as

$$\begin{aligned} \text{GLRT}(\mathbf{y}) &= \mathbf{L}_4(\hat{\tau}, \hat{f}_d) = \sqrt{b(\hat{\tau}, \hat{f}_d)} \\ &= |\mathbf{y}^H \mathbf{A}^{-1} \mathbf{\Phi} \mathbf{s}_r(\hat{\tau}, \hat{f}_d)| \\ &\geq \text{Th} \triangleq \frac{\sqrt{a(\hat{\tau}, \hat{f}_d)\sigma_\alpha^2 + 1}}{\sigma_\alpha} \\ &\quad \times \sqrt{\ln\left(\frac{p_0}{1 - p_0} (a(\hat{\tau}, \hat{f}_d)\sigma_\alpha^2 + 1)\right)}. \end{aligned} \quad (32)$$

(32) is the same as (8).

APPENDIX C

FINDING $f(z|H_1)$ IN SECTION IV

The starting point is (12) in Section IV, i.e.

$$f(z|H_1, \alpha) = \mathcal{CN}(\alpha a(\hat{\tau}, \hat{f}_d), a(\hat{\tau}, \hat{f}_d)). \quad (33)$$

By integrating (33) over the PDF of α , $f(z|H_1)$ can be found as

$$\begin{aligned} f(z|H_1) &= \int f(z|H_1, \alpha) f_\alpha(\alpha) d\alpha_r d\alpha_i \\ &= \frac{1}{\pi a(\hat{\tau}, \hat{f}_d) \pi \sigma_\alpha^2} \iint_{-\infty}^{\infty} \exp\left\{-\frac{|z - \alpha a(\hat{\tau}, \hat{f}_d)|^2}{a(\hat{\tau}, \hat{f}_d)}\right\} \\ &\quad \times \exp\left\{-\frac{|\alpha|^2}{\sigma_\alpha^2}\right\} d\alpha_r d\alpha_i, \end{aligned} \quad (34)$$

where α_r and α_i are as in A. The integration can be computed as

$$\begin{aligned} f(z|H_1) &= \frac{1}{\pi a(\hat{\tau}, \hat{f}_d) \pi \sigma_\alpha^2} \exp\left\{-\frac{|z|^2}{a(\hat{\tau}, \hat{f}_d)}\right\} \\ &\quad \times \iint_{-\infty}^{\infty} \exp\left\{-\left(a(\hat{\tau}, \hat{f}_d) + \frac{1}{\sigma_\alpha^2}\right)|\alpha|^2\right\} \exp\{z^* \alpha\} \\ &\quad \times \exp\{z \alpha^*\} d\alpha_r d\alpha_i = \frac{1}{\pi a(\hat{\tau}, \hat{f}_d) \pi \sigma_\alpha^2} \exp\left\{-\frac{|z|^2}{a(\hat{\tau}, \hat{f}_d)}\right\} \\ &\quad \times \iint_{-\infty}^{\infty} \exp\left\{-e(\hat{\tau}, \hat{f}_d) \left(|\alpha|^2 - \frac{z^* \alpha}{e(\hat{\tau}, \hat{f}_d)} - \frac{z \alpha^*}{e(\hat{\tau}, \hat{f}_d)}\right)\right\} \\ &\quad d\alpha_r d\alpha_i \\ &= \frac{1}{\pi a(\hat{\tau}, \hat{f}_d) \pi \sigma_\alpha^2} \exp\left\{-\frac{|z|^2}{a(\hat{\tau}, \hat{f}_d)}\right\} \iint_{-\infty}^{\infty} \exp\left\{-e(\hat{\tau}, \hat{f}_d)\right. \\ &\quad \times \left(|\alpha|^2 - \frac{z^* \alpha}{e(\hat{\tau}, \hat{f}_d)} - \frac{z \alpha^*}{e(\hat{\tau}, \hat{f}_d)}\right)\} d\alpha_r d\alpha_i = \frac{1}{\pi a(\hat{\tau}, \hat{f}_d) \pi \sigma_\alpha^2} \\ &\quad \times \exp\left\{-\frac{|z|^2}{a(\hat{\tau}, \hat{f}_d)}\right\} \iint_{-\infty}^{\infty} \exp\left\{-e(\hat{\tau}, \hat{f}_d) \left|\alpha - \frac{z}{e(\hat{\tau}, \hat{f}_d)}\right|^2\right. \\ &\quad \left.- \frac{|z|^2}{e^2(\hat{\tau}, \hat{f}_d)}\right)\} d\alpha_r d\alpha_i = \frac{1}{\pi a(\hat{\tau}, \hat{f}_d) \pi \sigma_\alpha^2} \exp\left\{-\frac{|z|^2}{a(\hat{\tau}, \hat{f}_d)}\right\} \\ &\quad \times \exp\left\{\frac{|z|^2}{e(\hat{\tau}, \hat{f}_d)}\right\} \iint_{-\infty}^{\infty} \exp\left\{-e(\hat{\tau}, \hat{f}_d) \left|\alpha - \frac{z}{e(\hat{\tau}, \hat{f}_d)}\right|^2\right\} \\ &\quad d\alpha_r d\alpha_i \\ &= \frac{1}{\pi a(\hat{\tau}, \hat{f}_d) \pi \sigma_\alpha^2} \exp\left\{-\frac{|z|^2}{a(\hat{\tau}, \hat{f}_d) e(\hat{\tau}, \hat{f}_d) \sigma_\alpha^2}\right\} \pi e(\hat{\tau}, \hat{f}_d) \\ &= \frac{1}{\pi a(\hat{\tau}, \hat{f}_d) \left(a(\hat{\tau}, \hat{f}_d) \sigma_\alpha^2 + 1\right)} \\ &\quad \times \exp\left\{-\frac{|z|^2}{a(\hat{\tau}, \hat{f}_d) \left(a(\hat{\tau}, \hat{f}_d) \sigma_\alpha^2 + 1\right)}\right\} \\ &= \mathcal{CN}\left(0, a(\hat{\tau}, \hat{f}_d) + a(\hat{\tau}, \hat{f}_d)^2 \sigma_\alpha^2\right). \end{aligned} \quad (35)$$

In (35), $e(\tau, f_d)$ is the same as defined in A.

REFERENCES

- [1] V. M. Patel, G. R. Easley, D. M. Healy, and R. Chellappa, "Compressed synthetic aperture radar," *Selected Topics in Signal Processing, IEEE Journal of*, vol. 4, no. 2, pp. 244–254, 2010.
- [2] A. Budillon, A. Evangelista, and G. Schirinzi, "Three-dimensional SAR focusing from multipass signals using compressive sampling," *Geoscience and Remote Sensing, IEEE Transactions on*, vol. 49, no. 1, pp. 488–499, 2011.

- [3] A. S. Khwaja and J. Ma, "Applications of compressed sensing for SAR moving-target velocity estimation and image compression," *Instrumentation and Measurement, IEEE Transactions on*, vol. 60, no. 8, pp. 2848–2860, 2011.
- [4] Y. Yu, A. P. Petropulu, and H. V. Poor, "MIMO radar using compressive sampling," *Selected Topics in Signal Processing, IEEE Journal of*, vol. 4, no. 1, pp. 146–163, 2010.
- [5] S. Gogineni and A. Nehorai, "Target estimation using sparse modeling for distributed MIMO radar," *Signal Processing, IEEE Transactions on*, vol. 59, no. 11, pp. 5315–5325, 2011.
- [6] Y. Yu, A. P. Petropulu, and H. V. Poor, "Measurement matrix design for compressive sensing-based MIMO radar," *Signal Processing, IEEE Transactions on*, vol. 59, no. 11, pp. 5338–5352, 2011.
- [7] R. G. Vaughan, N. L. Scott, and D. R. White, "The theory of bandpass sampling," *Signal Processing, IEEE Transactions on*, vol. 39, no. 9, pp. 1973–1984, 1991.
- [8] D. L. Donoho, "Compressed sensing," *Information Theory, IEEE Transactions on*, vol. 52, no. 4, pp. 1289–1306, 2006.
- [9] E. J. Candès, "Compressive sampling," in *Proceedings of the International Congress of Mathematicians: Madrid, August 22-30, 2006: invited lectures*, 2006, pp. 1433–1452.
- [10] R. G. Baraniuk, "Compressive sensing [lecture notes]," *Signal Processing Magazine, IEEE*, vol. 24, no. 4, pp. 118–121, 2007.
- [11] J. A. Tropp and A. C. Gilbert, "Signal recovery from random measurements via orthogonal matching pursuit," *Information Theory, IEEE Transactions on*, vol. 53, no. 12, pp. 4655–4666, 2007.
- [12] D. Needell and J. A. Tropp, "CoSaMP: Iterative signal recovery from incomplete and inaccurate samples," *Applied and Computational Harmonic Analysis*, vol. 26, no. 3, pp. 301–321, 2009.
- [13] T. Huang, Y. Liu, and X. Wang, "Adaptive subspace pursuit and its application in motion compensation for step frequency radar."
- [14] B. Zhang, X. Cheng, N. Zhang, Y. Cui, Y. Li, and Q. Liang, "Sparse target counting and localization in sensor networks based on compressive sensing," in *INFOCOM, 2011 Proceedings IEEE*. IEEE, 2011, pp. 2255–2263.
- [15] M. A. Davenport, P. T. Boufounos, M. B. Wakin, and R. G. Baraniuk, "Signal processing with compressive measurements," *Selected Topics in Signal Processing, IEEE Journal of*, vol. 4, no. 2, pp. 445–460, 2010.
- [16] M. C. Wicks, H. Kung, and H.-C. Chen, "Compressed statistical testing and application to radar," *1st International Workshop on Compressed Sensing applied to Radar*, Bonn, Germany, 14–16 May 2012 (<http://workshops.fhr.fraunhofer.de>).
- [17] C. W. Lim and M. B. Wakin, "Automatic modulation recognition for spectrum sensing using nonuniform compressive samples," in *Communications (ICC), 2012 IEEE International Conference on*. IEEE, 2012, pp. 3505–3510.
- [18] —, "CHOCS: a framework for estimating compressive higher order cyclostationary statistics," in *SPIE Defense, Security, and Sensing*. International Society for Optics and Photonics, 83650M, 2012.
- [19] Q. He, N. H. Lehmann, R. S. Blum, and A. M. Haimovich, "MIMO radar moving target detection in homogeneous clutter," *Aerospace and Electronic Systems, IEEE Transactions on*, vol. 46, no. 3, pp. 1290–1301, 2010.
- [20] M. I. Skolnik, *Introduction to radar systems*. Chapter 2, Section 2.8, p. 66, McGraw hill New York, 3rd edition, 2001.
- [21] E. Fishler, A. Haimovich, R. S. Blum, L. J. Cimini Jr, D. Chizhik, and R. A. Valenzuela, "Spatial diversity in radars-models and detection performance," *Signal Processing, IEEE Transactions on*, vol. 54, no. 3, pp. 823–838, 2006.
- [22] M. Jiang, R. Niu, and R. S. Blum, "Bayesian target location and velocity estimation for multiple-input multiple-output radar," *Radar, Sonar & Navigation, IET*, vol. 5, no. 6, pp. 666–670, 2011.
- [23] A. Papoulis and S. U. Pillai, *Probability, random variables, and stochastic processes*. Chapter 7, Section 7-2, pp. 258–259, Tata McGraw-Hill Education, 4th edition, 2002.
- [24] —, *Probability, random variables, and stochastic processes*. Chapter 6, Section 6-2, pp. 190–191, Tata McGraw-Hill Education, 4th edition, 2002.
- [25] K. B. Petersen and M. S. Pedersen, "The matrix cookbook," Chapter 8, Section 8.1, Subsection 8.1.1, p. 39, 2008.